ISSN 2070-0482, Mathematical Models and Computer Simulations, 2026, Vol. 18, No. 4, pp. 455–465. © Pleiades Publishing, Ltd., 2026.
Russian Text © The Author(s), 2026, published in Matematicheskoe Modelirovanie, 2026, Vol. 38, No. 2, pp. 49–64.

Reconstruction and Visualization of Electromagnetic Properties of a Three-Dimensional Body by Microwave Tomography

V. Yu. Martynova[a],* and M. Yu. Medvedik[a],**

[a] *Penza State University, Penza, Russia*

**e-mail: lynxbax@mail.ru*

***e-mail: medv@mail.ru*

Received October 13, 2025; revised October 13, 2025; accepted November 17, 2025

Abstract—This study analyzes the behavior of electromagnetic fields near bodies located in free space is considered and solves the inverse problem of restoring the characteristics of the bodies themselves on the basis of external field measurement data. This is of practical significance due to applications in medicine, flaw detection, and engineering. This paper consists of two subproblems. First, the direct problem is solved that describes the interaction of electromagnetic waves with the body, allowing one to establish regularities of changes in the field. Next, the obtained data are used to restored the electromagnetic properties of the body on the basis of external measurements. This algorithm includes a two-stage method, which is reduced to solving singular integral equations and a recalculation formula. The numerical simulation performed by us showed the model efficiency. Even at a noise level of 0.5%, we have managed to efficiently restore the parameters of inhomogeneities, reliably determining their shape and position. The approach is shown to be suitable in practice. Despite possible deviations in initial data, the algorithm provides stable and accurate results, allowing it to be used in real technology for nondestructive testing of materials, medical examinations, and environmental safety.

Keywords: three-dimensional vector inverse diffraction problem, restoration of dielectric constant, integro-differential equation, two-step method, numerical method

DOI: 10.1134/S2070048226700158

INTRODUCTION

Microwave tomography is an innovative method for studying the internal structures of objects by analyzing the passage of microwaves through the substance under study. It is becoming one of the most promising technologies due to its capability to effectively analyze the properties of materials and detect hidden changes and damage. This method is actively used in medicine, geophysics, materials science, and other fields of science and technology [1–5].

The main idea of the method is as follows. The object under study is placed between two (transmitting and receiving) antenna arrays. The transmitting antenna emits radio signals of a certain frequency, which pass through the body, interacting with the internal structures of the material. These signals are absorbed and scattered depending on the properties of the substance inside the object. Then, the receiving antenna records the weakened and distorted waves that have passed through the object.

To process the data obtained, we use a special computer program capable of converting the collected signals into an image of the internal structure of the object. This is done by calculating the distribution of the electromagnetic characteristics of the medium (such as permittivity) on the basis of the received signal intensity and phase. This allows us to identify heterogeneities and anomalies in the distribution of physical parameters in the body [6–9].

Microwave tomography has the advantages that it can detect hidden defects and structural irregularities in objects using relatively low levels of radiation energy. The method is highly sensitive to changes in the electrical properties of substances, making it successfully used for diagnosing soft tissue diseases, identifying defects in composites and polymers, monitoring underground resources, and studying environmental conditions.

However, microwave tomography is associated with a number of difficulties, including problems with measurement accuracy and interpretation of results. The nonlinearity of the processes of interaction between waves and matter leads to difficulties in restoring the true values of the parameters of the medium.

However, modern computational methods and algorithms make it possible to significantly improve the accuracy of image reconstruction, making this method increasingly requested in various fields of human activity.

1. STATEMENT OF THE DIRECT PROBLEM

Let us consider a rectangular parallelepiped $Q \subset \mathbb{R}^3$. The environment $\mathbb{R}^3 \backslash \bar{Q}$ is assumed to be isotropic and homogeneous with constant electrodynamic parameters $\varepsilon_0 > 0$, $\mu_0 > 0$, where ε_0 and μ_0 are the dielectric and magnetic permeability of vacuum, respectively. In this case, the body of Q is isotropic and nonuniform. The diffuser material of Q characterized by $\mu = \mu_0$ and the permittivity function $\varepsilon(r)$, where $r = (x, y, z)$. Let us introduce a complex-valued function associated with the heterogeneity of the given rectangular parallelepiped:

$$\xi(r) = \varepsilon_0(\varepsilon(r) - \varepsilon_0)^{-1} \tag{1}$$

for all points $r \in \bar{Q}$.

The source at point $r_s \in \mathbb{R}^3 \backslash \bar{Q}$ creates an electromagnetic wave $\mathbf{E}_0, \mathbf{H}_0 \in C^\infty(\mathbb{R}^3 \backslash r_s)$, the components of which are the solution of Maxwell's equations

$$\operatorname{curl} \mathbf{H}_0 = -i\omega\varepsilon_0\mathbf{E}_0, \quad \operatorname{curl} \mathbf{E}_0 = i\omega\mu_0\mathbf{H}_0. \tag{2}$$

Let $\mathbf{E}_s, \mathbf{H}_s$ be the components of the scattered field. The total field can be represented as

$$\mathbf{E} = \mathbf{E}_0 + \mathbf{E}_s, \quad \mathbf{H} = \mathbf{H}_0 + \mathbf{H}_s. \tag{3}$$

The solution to the direct diffraction problem is the total electromagnetic field $\mathbf{E}$, $\mathbf{H}$, satisfying in $\mathbb{R}^3 \backslash \bar{Q}$ Maxwell's equations

$$\operatorname{curl} \mathbf{H} = -i\omega\varepsilon\mathbf{E}, \quad \operatorname{curl} \mathbf{E} = i\omega\mu_0\mathbf{H}, \tag{4}$$

conditions of continuity of tangent components on the boundary of the heterogeneity domain:

$$[\mathbf{E}_\tau]\big|_{\partial Q} = [\mathbf{H}_\tau]\big|_{\partial Q} = 0, \tag{5}$$

conditions of finite energy in any limited volume of space:

$$\mathbf{E}, \mathbf{H} \in \mathbf{L}_{2,\mathrm{loc}}(\mathbb{R}^3). \tag{6}$$

Silver–Müller radiation conditions [10] at infinity for the scattered field:

$$\begin{gathered} \mathbf{H}_s \times \mathbf{e}_r - \mathbf{E}_s = o(r^{-1}) \mathbf{E}_s \times \mathbf{e}_r + \mathbf{H}_s = o(r^{-1}), \\ \mathbf{E}_s, \mathbf{H}_s = O(r^{-1}), \quad r \to \infty, \end{gathered} \tag{7}$$

where $\mathbf{e}_r = \mathbf{x}/|\mathbf{x}|$, $\mathbf{x} = (x_1, x_2, x_3)^T$,

$$\mathbf{E}, \mathbf{H} \in C^2(\mathbb{R}^3 \backslash \partial Q) \cap C(\bar{Q}) \cap C(\mathbb{R}^3 \backslash Q). \tag{8}$$

It should be noted that the limit relations in (7) are satisfied uniformly in all directions.

Definition 1. Solution $\mathbf{E}, \mathbf{H}$ of problem (2)–(7), satisfying conditions (8) is called a classical solution.

The following results on the solvability of the direct diffraction problem can be found in [11].

Proposition 1. *Let dielectric permittivity satisfy the following conditions in* $\bar{Q}$:

$$\varepsilon \in C^\infty(\bar{Q}), \quad \operatorname{Re} \varepsilon > \varepsilon_0, \quad \operatorname{Im} \varepsilon \geq 0, \tag{9}$$

and $\varepsilon = \varepsilon_0$ *and* $\mu = \mu_0$ *outside* $\bar{Q}$. *Then*, *diffraction problem* (2)–(8) *has no more than one classical solution*.

Boundary value problem (2)–(8) can be reduced to a system consisting of an integro-differential equation over the inhomogeneity domain:

$$\mathbf{E}_0(r) = \mathbf{E}(r) - (k_0^2 + \operatorname{grad}\operatorname{div})\int_Q G(r, r_0)(\xi(r_0))^{-1}\mathbf{E}(r_0)dr_0, \quad r \in Q, \tag{10}$$

and the integral representation of the field outside the body:

$$\mathbf{E}_0(r) = \mathbf{E}(r) - (k_0^2 + \operatorname{grad}\operatorname{div})\int_Q G(r, r_0)(\xi(r_0))^{-1}\mathbf{E}(r_0)dr_0, \quad r \in \mathbb{R}^3\backslash\bar{Q}, \tag{11}$$

where $k_0^2 = \omega^2\varepsilon_0\mu_0$ is the wave number of free space, the Green function has the form $G(r, r_0) = \exp(ik_0|r - r_0|)/(4\pi|r - r_0|)$, and the incident field is calculated using the Green function with one fixed point $r_s \in \mathbb{R}^3\backslash\bar{Q}$, determining the source location $\mathbf{E}_0(r) = G(r, r_s)$.

The magnetic field is everywhere expressed in terms of the electric field according to the formula

$$\mathbf{H} = \frac{1}{i\omega\mu_0}\operatorname{curl}\mathbf{E}. \tag{12}$$

There holds a theorem on the equivalence of a boundary value problem and an integro–differential equation.

Proposition 2. *If boundary value problem* (2)–(8) *has a classical solution* **E**, **H**, *then the vector function* $\mathbf{E} \in C(\bar{Q}) \cap \mathbf{L}_2(Q)$ *satisfies integro–differential equation* (11). *Conversely, if* $\mathbf{E} \in \mathbf{L}_2(Q)$ *satisfies Eq.* (11), *then boundary value problem* (2)–(8) *has a classical solution* **E**, **H**, *expressed by formulas* (10)–(12).

Proposition 3. *Let dielectric permittivity satisfy conditions* (9) *for* $r \in \bar{Q}$. *Then, the operator*

$$A\mathbf{E}(r) := \mathbf{E}(r) - (k_0^2 + \operatorname{grad}\operatorname{div})\int_Q G(r, r_0)(\xi(r_0))^{-1}\mathbf{E}(r_0)dr_0$$

is continuously invertible in $\mathbf{L}_2(Q)$.

The proofs of Propositions 1–3 can be found in [12, 13].

2. STATEMENT OF THE INVERSE PROBLEM

Let us consider the vector inverse problem of reconstructing the inhomogeneity of an isotropic dielectric body:

$$Q := \{r = (x, y, z): 0 \le x \le R_x, 0 \le y \le R_y, 0 \le z \le R_z\},$$

characterized by a wave number $k_0 > 0$, where $R_x > 0$, $R_y > 0$, $R_z > 0$ are the lengths of the edges of the rectangular parallelepiped. The geometry of the problem is shown in Fig. 1.

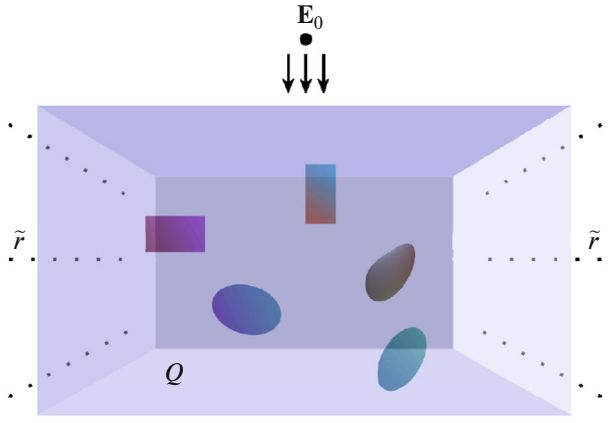


Fig. 1. Heterogeneous body Q in the form of a rectangular parallelepiped, observation points $\tilde{r}$ located outside the body, source of the field $\mathbf{E}_0$, and heterogeneities of various shapes and sizes.

Let us construct on the body Q a uniform computational grid with nodes

$$x_{i_1} = \frac{R_x}{n_1} i_1, \quad y_{i_2} = \frac{R_y}{n_2} i_2, \quad z_{i_3} = \frac{R_z}{n_3} i_3, \quad i_k = \overline{0, n_k}, \quad k = 1,2,3,$$

where $n_k + 1$ is the number of nodes of the computational grid in the kth direction, $k = 1, 2, 3$. In line with this calculation grid, the body Q consists of elementary cells $Q_{i_1 i_2 i_3} = \{r: x_{i_1} < x < x_{i_1+1}, y_{i_2} < y < y_{i_2+1}, z_{i_3} < z < z_{i_3+1}\}$, $i_k = \overline{0, n_k - 1}$, $k = 1, 2, 3$.

Let us introduce piecewise constant functions

$$\chi_{i_1 i_2 i_3}(r) = \begin{cases} 1, & r \in Q_{i_1 i_2 i_3} \\ 0, & r \notin Q_{i_1 i_2 i_3} \end{cases} \tag{13}$$

and assume that the domain Q is characterized by constant magnetic permeability $\mu_0 > 0$ and the piecewise constant function of dielectric permittivity $\varepsilon(r)$ to be found. More precisely,

$$\varepsilon(r) = \left\{\varepsilon_{i_1 i_2 i_3}, \quad r \in Q_{i_1 i_2 i_3}, \quad i_k = \overline{0, n_k - 1}, \quad k = 1,2,3.\right.$$

Dielectric permittivity at the points of faces $\partial Q_{i_1 i_2 i_3}$ can be further defined as a limit of values $\varepsilon(r)$ in one of the adjacent cells.

Introducing a multi-index $\mathbf{i} = (i_1 i_2 i_3)$, we represent the function $\varepsilon(r)$ at each $r \in Q$ as

$$\varepsilon(r) = \sum_{\mathbf{i}} \varepsilon_{\mathbf{i}} \chi_{\mathbf{i}}(r).$$

Let some limited domain of space D be given such that $\overline{D} \cap \overline{Q} = \varnothing$, within which the full field of a certain frequency $\omega > 0$ is considered. Field values are measured either experimentally (using physical instruments and sensors in a real environment) or theoretically (by numerical modeling of the direct problem described earlier).

It is assumed that the value of the given field of a given frequency is known exactly at all points $r \in D$. These data allow us to analyze field properties and solve inverse problems that reconstruct unknown characteristics of the medium, such as the distribution of sources or material properties. They can be simulated or obtained using special equipment. It should be noted that the accuracy of reconstructing the environmental parameters depends on the density of the measurement points and the sensitivity of the equipment used. The greater is the number of observations and the more accurate are the sensors, the better is the quality of reconstruction of initial parameters of the model.

To formulate the inverse diffraction problem, we use the system of integral equalities (10), (11), which describe the dependence of the field $\mathbf{E}(x)$ on dielectric permittivity $\varepsilon(r)$ and the incident wave $\mathbf{E}_0(r)$.

Definition 2. The inverse problem of diffraction consists is to reconstruct the function $\varepsilon(r)$ in the inhomogeneity domain Q from measured total field $\mathbf{E}(r)$ at the points of D, using the equality

$$\mathbf{E}_0(r) = \mathbf{E}(r) - (k_0^2 + \operatorname{grad}\operatorname{div}) \int_Q G(r, r_0)(\xi(r_0))^{-1} \mathbf{E}(r_0) dr_0, \quad r \in D, \tag{14}$$

taking into account the equation in the inhomogeneity domain Q:

$$\mathbf{E}_0(r) = \mathbf{E}(r) - (k_0^2 + \operatorname{grad}\operatorname{div}) \int_Q G(r, r_0)(\xi(r_0))^{-1} \mathbf{E}(r_0) dr_0, \quad r \in Q. \tag{15}$$

Let us describe a two-step method for solving the inverse diffraction problem. First, we introduce a vector function $\mathbf{J}(r)$ on Q as

$$\mathbf{J}(r) := (\xi(r))^{-1} \mathbf{E}(r),$$

where the function $\xi(r)$ is determined by formula (1). We assume that the condition is satisfied everywhere for $r \in \overline{Q}$. In the new notation, the representation of the field outside scatterer (14) has the form

$$(k_0^2 + \operatorname{grad}\operatorname{div}) \int_Q G(r, r_0) \mathbf{J}(r_0) dr_0 = \mathbf{E}(r) - \mathbf{E}_0(r), \quad r \in D, \tag{16}$$

and the equation for points inside body (15) can be rewritten as

$$\xi(r)\mathbf{J}(r) - (k_0^2 + \operatorname{grad}\operatorname{div})\int_Q G(r,r_0)\mathbf{J}(r_0)dr_0 = \mathbf{E}_0(r), \quad r \in Q. \tag{17}$$

The two-step method for reconstructing the structure of the given body Q can be described as follows. In the first step, Eq. (16) is used to determine the value of current $\mathbf{J}(r)$ in Q, where the values of the incident $\mathbf{E}_0(r)$ and complete $\mathbf{E}(r)$ fields in the domain D located outside Q are known. The first step is the most difficult, since one has to solve a volume singular integral equation of the first kind. Since the solution of such equations leads to the appearance of ill-conditioned matrices, regularization procedures for the problem are required. At the second step, formula (17) is used to determine the values of the function $\xi(r)$ using in the diffuser Q. The values of dielectric permittivity $\varepsilon(r)$ of Q are uniquely restored from the known values of $\xi(r)$ using the formula

$$\varepsilon(r) = \varepsilon_0 + \varepsilon_0\left(\xi(r)\right)^{-1}.$$

The authors of [11] proved the uniqueness of the solution of such an inverse problem. This approach allows one to consecutively restore the internal structure of an object, taking into account the complex relationship between electric fields and the material characteristics of the media under consideration.

3. NUMERICAL METHOD

Both direct and inverse problems are solved by the collocation method, which requires the selection of basis functions and collocation points. The studies [14–17] implemented the method with basis functions of form (13) with a support that is limited to one elementary cell. However, this approach does not allow the divergence operation to be taken under the integral sign and applied to the basis function, which leads to a singular integro–differential equation. This necessitates the use of special methods for processing the singularities of integrals.

Smolkin and Smirnov (2024) proposed three types of basis functions [18]:

$$v_{\mathbf{i}}^{(x)}(r) = \begin{cases} 1 - \left|x - x_{i_1}\right|/h_1, & r \in Q_{i_1i_2i_3} \cup Q_{i_1+1i_2i_3}, \\ 0, & r \notin Q_{i_1i_2i_3} \cup Q_{i_1+1i_2i_3}, \end{cases} \tag{18}$$
$$i_1 = \overline{0, n_1 - 2}, \quad i_k = \overline{0, n_k - 1}, \quad k = 2,3,$$

$$v_{\mathbf{i}}^{(y)}(r) = \begin{cases} 1 - \left|y - y_{i_2}\right|/h_2, & r \in Q_{i_1i_2i_3} \cup Q_{i_1i_2+1i_3}, \\ 0, & r \notin Q_{i_1i_2i_3} \cup Q_{i_1i_2+1i_3}, \end{cases} \tag{19}$$
$$i_2 = \overline{0, n_2 - 2}, \quad i_k = \overline{0, n_k - 1}, \quad k = 1,3,$$

$$v_{\mathbf{i}}^{(z)}(r) = \begin{cases} 1 - \left|z - z_{i_3}\right|/h_3, & r \in Q_{i_1i_2i_3} \cup Q_{i_1i_2i_3+1}, \\ 0, & r \notin Q_{i_1i_2i_3} \cup Q_{i_1i_2i_3+1}, \end{cases} \tag{20}$$
$$i_3 = \overline{0, n_3 - 2}, \quad i_k = \overline{0, n_k - 1}, \quad k = 1,2.$$

The use of the specified basis functions leads to the appearance of integrals exclusively with weak singularities. It should be noted that the supports of functions (18)–(20) cover two adjacent elementary cells.

When implementing the collocation method, it is necessary to calculate the integrals

$$(k_0^2 + \operatorname{grad}\operatorname{div})\int_Q G(r,r_0)\tilde{\mathbf{J}}(r_0)dr_0,$$

where $\tilde{\mathbf{J}}$ is an approximate solution.

First, we write the formula for calculating the gradient in the form

$$\operatorname{grad}_r G(r,r_0) = g\left(|r - r_0|\right)\left((x - x_0)\,\mathbf{x} + (y - y_0)\,\mathbf{y} + (z - z_0)\,\mathbf{z}\right), \tag{21}$$

where $g(t) \coloneqq (ik_0 - 1/t)\exp(ik_0t)/(4\pi t^2)$.

Let us find formulas for calculating divergence using vector basis functions

$$\begin{aligned}
&\mathbf{v}_{\mathbf{i}}^{(x)}(r) = v_{\mathbf{i}}^{(x)}(r)\mathbf{x}(r), \quad i_1 = \overline{0, n_1 - 2}, \quad i_k = \overline{0, n_k - 1}, \ k = 2,3,\\
&\mathbf{v}_{\mathbf{i}}^{(y)}(r) = v_{\mathbf{i}}^{(y)}(r)\mathbf{y}(r), \quad i_2 = \overline{0, n_2 - 2}, \quad i_k = \overline{0, n_k - 1}, \ k = 1,3,\\
&\mathbf{v}_{\mathbf{i}}^{(z)}(r) = v_{\mathbf{i}}^{(z)}(r)\mathbf{z}(r), \quad i_3 = \overline{0, n_3 - 2}, \quad i_k = \overline{0, n_k - 1}, \ k = 1,2,
\end{aligned} \tag{22}$$

where $\mathbf{x}$, $\mathbf{y}$, $\mathbf{z}$ are unit vectors in the corresponding directions. Then, within the limits of their supports, we calculate the divergence of basis functions (22), using formulas (18)–(20):

$$\begin{aligned}
&\operatorname{div} \mathbf{v}_{\mathbf{i}}^{(x)}(r) = -\operatorname{sgn}(x - x_{i_1})/h_1, \quad i_1 = \overline{0, n_1 - 2}, \quad i_k = \overline{0, n_k - 1}, \quad k = 2,3,\\
&\operatorname{div} \mathbf{v}_{\mathbf{i}}^{(y)}(r) = -\operatorname{sgn}(y - y_{i_2})/h_2, \quad i_2 = \overline{0, n_2 - 2}, \quad i_k = \overline{0, n_k - 1}, \quad k = 1,3,\\
&\operatorname{div} \mathbf{v}_{\mathbf{i}}^{(z)}(r) = -\operatorname{sgn}(z - z_{i_3})/h_3, \quad i_3 = \overline{0, n_3 - 2}, \quad i_k = \overline{0, n_k - 1}, \quad k = 1,2,
\end{aligned} \tag{23}$$

and at points that do not belong to the supports, the divergences are equal to zero. Due to the specificity of the basis functions, divergences from them are found in a standard way, rather than as generalized functions, and are piecewise continuous.

It is convenient to search the approximate solution $\tilde{\mathbf{J}}$ in the form

$$\tilde{\mathbf{J}}(r) = \tilde{\mathbf{J}}^{(x)}(r) + \tilde{\mathbf{J}}^{(y)}(r) + \tilde{\mathbf{J}}^{(z)}(r), \tag{24}$$

where $\tilde{\mathbf{J}}^{(x)}$, $\tilde{\mathbf{J}}^{(y)}$, $\tilde{\mathbf{J}}^{(z)}$ are linear combinations of the corresponding basis functions with unknown coefficients:

$$\begin{aligned}
&\tilde{\mathbf{J}}^{(x)}(r) = \sum_{\mathbf{i}} J_{\mathbf{i}}^{(x)} \mathbf{v}_{\mathbf{i}}^{(x)}(r), \quad i_1 = \overline{0, n_1 - 2}, \quad i_k = \overline{0, n_k - 1}, \quad k = 2,3,\\
&\tilde{\mathbf{J}}^{(y)}(r) = \sum_{\mathbf{i}} J_{\mathbf{i}}^{(y)} \mathbf{v}_{\mathbf{i}}^{(y)}(r), \quad i_2 = \overline{0, n_2 - 2}, \quad i_k = \overline{0, n_k - 1}, \quad k = 1,3,\\
&\tilde{\mathbf{J}}^{(z)}(r) = \sum_{\mathbf{i}} J_{\mathbf{i}}^{(z)} \mathbf{v}_{\mathbf{i}}^{(z)}(r), \quad i_3 = \overline{0, n_3 - 2}, \quad i_k = \overline{0, n_k - 1}, \quad k = 1,2.
\end{aligned} \tag{25}$$

It should be noted that the normal component of the approximate solution is vanishing on the boundary ∂Q at the points of smoothness of the boundary, $\tilde{\mathbf{J}}(r) \cdot \nu(r) = 0$, where $\nu(r)$ is the external normal to the boundary at $r \in \partial Q$. In addition, it is obvious that the introduced basis functions have the property of approximation in space $L_2(Q)$.

To implement the numerical method, it is necessary to calculate the divergence of the volume integral. The authors of [18] proved that

$$\operatorname{div}_r \int_Q G(r, r_0)\tilde{\mathbf{J}}(r_0)dr_0 = \int_Q G(r, r_0) \operatorname{div} \tilde{\mathbf{J}}(r_0)dr_0 \tag{26}$$

for any $r \in \mathbb{R}^3$.

Now, we calculate $\operatorname{grad}_r \operatorname{div}_r \int_Q G(r, r_0)\tilde{\mathbf{J}}(r_0)dr_0 = \int_Q \operatorname{grad}_r G(r, r_0) \operatorname{div} \tilde{\mathbf{J}}(r_0)dr_0$ already as an improper absolutely convergent integral, since the kernel singularity is of the order $O\left(|r - r_0|^{-2}\right)$ as $|r - r_0| \to 0$ (weak singularity). Using (21), (23), we obtain $\operatorname{grad}_r G(r, r_0)$ and $\operatorname{div} \tilde{\mathbf{J}}(r_0)$, respectively.

Finally, we have

$$\begin{aligned}
&(k_0^2 + \operatorname{grad}_r \operatorname{div}_r) \int_Q G(r, r_0)\tilde{\mathbf{J}}(r_0)dr_0\\
&= k_0^2 \int_0^{R_x} \int_0^{R_y} \int_0^{R_z} G(x, y, z, x_0, y_0, z_0)\tilde{\mathbf{J}}(x_0, y_0, z_0)dx_0dy_0dz_0\\
&+ \int_0^{R_x} \int_0^{R_y} \int_0^{R_z} \operatorname{grad} G(x, y, z, x_0, y_0, z_0) \operatorname{div} \tilde{\mathbf{J}}(x_0, y_0, z_0)dx_0dy_0dz_0.
\end{aligned}$$

In [18], three types of collocation points for the direct problem are proposed in the form

$$r_{\mathbf{i}}^{(x)} = (x_{i_1} + h_1, y_{i_2} + 0.5h_2, z_{i_3} + 0.5h_3), \quad i_1 = \overline{0, n_1 - 2}, \quad i_k = \overline{0, n_k - 1}, \quad k = 2,3,$$
$$r_{\mathbf{i}}^{(y)} = (x_{i_1} + 0.5h_1, y_{i_2} + h_2, z_{i_3} + 0.5h_3), \quad i_2 = \overline{0, n_2 - 2}, \quad i_k = \overline{0, n_k - 1}, \quad k = 1,3, \tag{27}$$
$$r_{\mathbf{i}}^{(x)} = (x_{i_1} + 0.5h_1, y_{i_2} + 0.5h_2, z_{i_3} + h_3), \quad i_3 = \overline{0, n_3 - 2}, \quad i_k = \overline{0, n_k - 1}, \quad k = 1,2.$$

In this approach, the collocation points correspond uniquely to the basis functions, and the number of nodes coincides with the number of basis functions, which forms a square matrix A of the system of linear algebraic equations

$$A\mathbf{c} = \mathbf{f}$$

in the collocation method, where $\mathbf{c}$ is the vector of unknown coefficients

$$J_{\mathbf{i}}^{(x)}, \quad i_1 = \overline{0, n_1 - 2}, \quad i_k = \overline{0, n_k - 1}, \quad k = 2,3,$$
$$J_{\mathbf{i}}^{(y)}, \quad i_2 = \overline{0, n_2 - 2}, \quad i_k = \overline{0, n_k - 1}, \quad k = 1,3, \tag{28}$$
$$J_{\mathbf{i}}^{(z)}, \quad i_3 = \overline{0, n_3 - 2}, \quad i_k = \overline{0, n_k - 1}, \quad k = 1,2,$$

$\mathbf{f}$ is the vector of the incident field at collocation points (27). The matrix A has a block structure of size 3×3, and its elements are determined by the relationship

$$a_{\mathbf{ij}}^{(\alpha\beta)} = \xi(r_{\mathbf{i}}^{(\alpha)}) v_{\mathbf{j}}^{(\beta)}(r_{\mathbf{i}}^{(\alpha)}) - k_0^2 \int_0^{R_x}\int_0^{R_y}\int_0^{R_z} G(r_{\mathbf{i}}^{(\alpha)}; x_0, y_0, z_0) v_{\mathbf{j}}^{(\beta)}(x_0, y_0, z_0) dx_0 dy_0 dz_0$$
$$- \int_0^{R_x}\int_0^{R_y}\int_0^{R_z} \operatorname{grad}^{(\alpha)} G(r_{\mathbf{i}}^{(\alpha)}; x_0, y_0, z_0) \operatorname{div} \mathbf{v}_{\mathbf{j}}^{(\beta)}(x_0, y_0, z_0) dx_0 dy_0 dz_0, \tag{29}$$

where $\mathbf{i} = (i_1 i_2 i_3)$, $\mathbf{j} = (j_1 j_2 j_3)$, are multi-indexes and $\operatorname{grad}^{(\alpha)}$ are the corresponding components of the gradient $\operatorname{grad} = \left(\operatorname{grad}^{(x)}, \operatorname{grad}^{(y)}, \operatorname{grad}^{(z)}\right)$, $\alpha,\beta = x, y, z$. In these chosen notations, the elements of vectors $\mathbf{c}$ and $\mathbf{f}$ have the form

$$c_{\mathbf{i}}^{(\alpha)} = J_{\mathbf{i}}^{(\alpha)}, \quad f_{\mathbf{i}}^{(\alpha)} = \mathbf{E}_0(r_{\mathbf{i}}^{(\alpha)}).$$

It should be noted that the upper bounds of the indices i_k, $k = 1,2,3$, in the multi-index $\mathbf{i} = (i_1 i_2 i_3)$ depend on direction α. Similarly, the upper bounds of the indices j_k, $k = 1,2,3$, in the multi-index $\mathbf{j} = (j_1 j_2 j_3)$ depend on direction β.

Thus, numerically solving the direct problem, we find the values of current $\tilde{\mathbf{J}}$ on the body Q, using (24), (25). The direct problem allows us to determine the electromagnetic field for further solution of the inverse problem. Using $\tilde{\mathbf{J}}$, we calculate the electromagnetic field using the formula

$$\mathbf{E}\left(\tilde{r}_{\mathbf{i}}^{(\alpha)}\right) = f_{\mathbf{i}}^{(\alpha)} + k_0^2 \int_0^{R_x}\int_0^{R_y}\int_0^{R_z} G(\tilde{r}_{\mathbf{i}}^{(\alpha)}; x_0, y_0, z_0) \tilde{\mathbf{J}}(x_0, y_0, z_0) dx_0 dy_0 dz_0$$
$$+ \int_0^{R_x}\int_0^{R_y}\int_0^{R_z} \operatorname{grad}^{(\alpha)} G(\tilde{r}_{\mathbf{i}}^{(\alpha)}; x_0, y_0, z_0) \operatorname{div} \tilde{\mathbf{J}}(x_0, y_0, z_0) dx_0 dy_0 dz_0$$

at selected observation points $\tilde{r}_{\mathbf{i}}^{(\alpha)} \in D$, $\alpha,\beta = x, y, z$. As before, the values of the upper bounds of i_k, $k = 1, 2, 3$, in a multi-index $\mathbf{i} = (i_1 i_2 i_3)$ depend on direction α. Observation points are located in several layers around the body Q at the same distance from its surface.

As mentioned above, the problem of restoring the heterogeneity of a body is solved in two stages. At the first stage, we obtain the system

$$\tilde{A}\mathbf{c} = \tilde{\mathbf{f}} - \mathbf{q}, \tag{30}$$

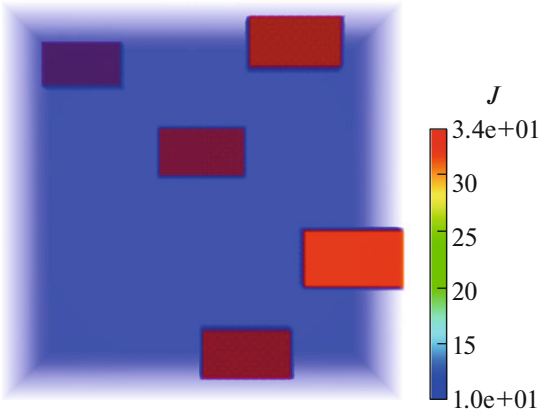


Fig. 2.

where are the elements of matrix $\tilde{A}$ have the form

$$\tilde{a}_{\mathbf{ij}}^{(\alpha\beta)} = -k_0^2 \int_0^{R_x}\int_0^{R_y}\int_0^{R_z} G(\tilde{r}_{\mathbf{i}}^{(\alpha)}; x_0, y_0, z_0) v_{\mathbf{j}}^{(\beta)}(x_0, y_0, z_0) dx_0 dy_0 dz_0$$

$$- \int_0^{R_x}\int_0^{R_y}\int_0^{R_z} \mathrm{grad}^{(\alpha)} G(\tilde{r}_{\mathbf{i}}^{(\alpha)}; x_0, y_0, z_0)\, \mathrm{div}\, \mathbf{v}_{\mathbf{j}}^{(\beta)}(x_0, y_0, z_0) dx_0 dy_0 dz_0,$$

the elements of vectors $\mathbf{q}$, $\tilde{\mathbf{f}}$ are

$$q_{\mathbf{i}}^{(\alpha)} = \mathbf{E}\left(\tilde{r}_{\mathbf{i}}^{(\alpha)}\right), \quad \tilde{f}_{\mathbf{i}}^{(\alpha)} = \mathbf{E}_0\left(\tilde{r}_{\mathbf{i}}^{(\alpha)}\right),$$

as in the direct problem, and $\mathbf{c}$ is the vector of unknown coefficients of (28). $\tilde{A}$ is a block matrix of size 3×3.

In the second step, we restore the value of ξ at collocation points (27), using the conversion formula

$$\xi\left(r_{\mathbf{i}}^{(\alpha)}\right) = \left(\sum_{\mathbf{i}}\sum_{\mathbf{j}} a_{\mathbf{ij}}^{(\alpha\beta)} J_{\mathbf{j}}^{(\beta)} + f_{\mathbf{i}}^{(\alpha)}\right)\left(\sum_{\mathbf{i}}\sum_{\mathbf{j}} V_{\mathbf{j}}^{(\beta)}\left(r_{\mathbf{i}}^{(\alpha)}\right) J_{\mathbf{j}}^{(\beta)}\right)^{-1}, \tag{31}$$

where $\alpha, \beta = x, y, z$.

4. NUMERICAL RESULTS

The distribution of irregularities of the rectangular parallelepiped Q is shown in Fig. 2. Figures 3–5 show the absolute values of the complex dielectric permittivity found using two-step method (30), (31) described in Section 3. The results were visualized using the freely distributed ParaView program. The radiation source is located at a distance from the surface outside the body Q and observation points, as shown in Fig. 1. The calculations were performed at a frequency of 100 GHz. For the calculations, a special case of a cube was chosen with an edge length of 0.1 m. For the given body Q, a regular computational grid was constructed. The number of divisions of the calculation grid in each direction is 8. The size of each matrix is 1344. The numerical experiments were performed at various frequencies of the microwave range.

The solutions of the inverse problem shown in Fig. 2–5 were obtained using noisy electromagnetic field data. The level of artificially added white noise is indicated in the captions to each figure.

Figure 3 shows the reconstructed values of the piecewise constant function of dielectric permittivity of the body Q, obtained using two-step method (30), (31), where white noise at a level of 0.1% was introduced into the results of the near field calculation. All 5 inclusions were found.

Figures 4 and 5 demonstrate the reconstructed values of the piecewise constant function of dielectric permittivity of the body Q, obtained using two-step method (30), (31), where white noise at a level of 0.5%

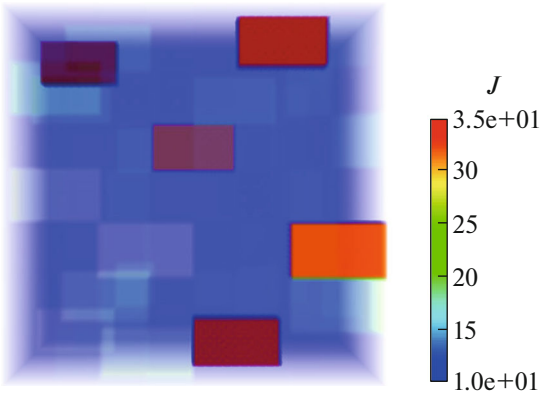


Fig. 3.

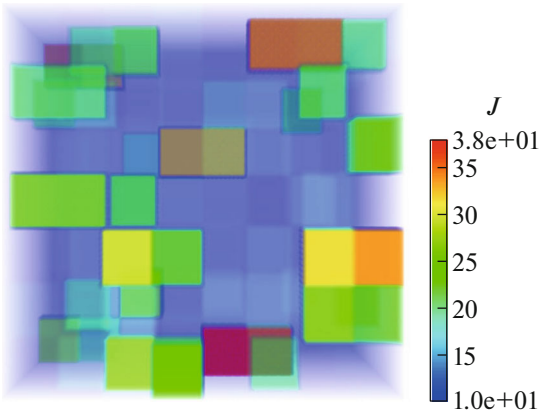


Fig. 4.

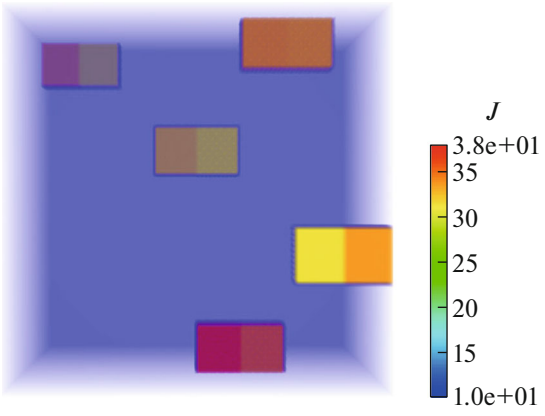


Fig. 5.

was introduced into the results of the near-field calculation. In Fig. 4, a large number of “artifacts” appeared. To suppress them, we used a filtration procedure, the results of which are presented in Fig. 5. To apply the filtering procedure, we solved the problem at different frequencies. All the artifacts moved from place to place, while the true heterogeneities retained their positions.

Thus, the numerical results show that introducing an error of 0.5% at the stage of measuring the electromagnetic field does not significantly affect the final reconstructed inhomogeneities in the given body.

The Matrix $\tilde{A}$ used in solving the inverse problem is ill-conditioned. Therefore, the regularization procedure [19] was used in the form

$$\left(\tilde{A}^*\tilde{A} + \gamma I\right)\mathbf{c} = \tilde{A}^*\left(\tilde{\mathbf{f}} - \mathbf{q}\right),$$

where I is the identity matrix. The value of the parameter γ is selected taking into account the specifics of the matrix $\tilde{A}$.

In this paper, the solutions of the direct problem are used to simulate the field values at observation points in the domain D. However, in practice, special devices are used to measure actual field values at observation points.

Calculations of the inverse acoustic problem using a two-step method for a hemisphere and a cylinder were performed in [20–22]. The solutions of direct and inverse electrodynamic problems using a two-step method for structures in the form of a rectangular parallelepiped are presented in [23, 24].

CONCLUSIONS

Numerical modeling of the inverse problem of reconstructing the body structure using a two-step method confirmed that even in the presence of random errors of the order of 0.5%, the values of the inhomogeneity parameters are reconstructed with a sufficient accuracy. In this case, the positions and forms of inhomogeneities are determined. Thus, the efficiency of the proposed approach was confirmed in practice.

Despite the presence of possible deviations in initial data, the method demonstrated good results in determining the characteristics of complex geometric shapes. The proposed approach can be applied to real devices used for nondestructive testing of materials, medical diagnostics, and environmental monitoring.

FUNDING

This work was supported by the Ministry of Science and Higher Education of the Russian Federation, state task no. 124020200015-7.

CONFLICT OF INTEREST

The authors of this work declare that they have no conflicts of interest.

REFERENCES

1. P. M. Meaney, Q. Fang, T. Rubaek, E. Demidenko, and K. D. Paulsen, "Log transformation benefits parameter estimation in microwave tomographic imaging," Med. Phys. **34** (6), 2014–2023 (2007).
2. P. M. Meaney, D. Goodwin, A. H. Golnabi, T. Zhou, M. Pallone, S. D. Geimer, G. Burke, and K. D. Paulsen, "Clinical microwave tomographic imaging of the calcaneus: A first-in-human case study of two subjects," IEEE Trans. Biomed. Eng. **59** (12), 3304–3313 (2012).
3. S. N. Semenov, "Imaging dielectric objects by microwave tomography," Nauchno-Tekh. Vedomosti S.-Peterb. Gos. Politekh. Univ., Ser. Fiz.-Mat. Nauki, No. 3, 150–155 (2015).
4. Z. Zhang, H. Liu, X. Gao, Z. Zhang, Z. S. He, L. Liu, R. Zong, and Z. Qin, "Two-step iterative medical microwave tomography," Sensors **24** (21), 6897 (2024).
5. V. Cherepenin, A. Karpov, A. Korjenevsky, V. Kornienko, A. Mazaletskaya, D. Mazourov, and D. Meister, "A 3D electrical impedance tomography (EIT) system for breast cancer detection," Physiol. Meas. **22** (1), 9–18 (2001).
6. V. G. Romanov, *Inverse Problems of Mathematical Physics* (Nauka, Moscow, 1984; De Gruyter, Berlin–Boston, 1986).
7. M. M. Lavrent'ev, V. G. Romanov, and S. P. Shishatskii, *Ill-Posed Problems of Mathematical Physics and Analysis* (Nauka, Moscow, 1980; American Mathematical Society, Providence, R.I., 1986).
8. A. B. Bakushinsky and A. V. Goncharsky, *Ill-Posed Problems: Theory and Applications* (Nauka, Moscow, 1989; Kluwer, Dordrecht, 1994).
9. A. N. Tikhonov, A. V. Goncharsky, V. V. Stepanov, and A. G. Yagola, *Numerical Methods for the Solution of Ill-Posed Problems* (Nauka, Moscow, 1990; Kluwer, Dordrecht, 1995).

10. D. Colton and R. Kress, *Inverse Acoustic and Electromagnetic Scattering Theory* (Springer, Berlin–Heidelberg, 2013).
11. Y. G. Smirnov, A. A. Tsupak, and M. Y. Medvedik, "Inverse vector problem of diffraction by inhomogeneous body with a piecewise smooth permittivity," J. Inverse Ill-Posed Probl. **32** (3), 453–465 (2024).
12. Y. G. Smirnov and A. A. Tsupak, "On the volume singular integro-differential equation for the electromagnetic diffraction problem," Appl. Anal. **96** (2), 173–189 (2017).
13. Yu. G. Smirnov and A. A. Tsupak, "Existence and uniqueness theorems in electromagnetic diffraction on systems of lossless dielectrics and perfectly conducting screens," Appl. Anal. **96** (8), 1326–1341 (2017).
14. M. Y. Medvedik, Y. G. Smirnov, and A. A. Tsupak, "Two-step method for solving inverse problem of diffraction by an inhomogeneous body," in *Nonlinear and Inverse Problems in Electromagnetics (PIERS 2017)*, Springer Proceedings in Mathematics and Statistics, Vol. 38 (Springer, 2018), pp. 83–92.
15. M. Y. Medvedik, Y. G. Smirnov, and A. A. Tsupak, "The two-step method for determining a piecewise-continuous refractive index of a 2D scatterer by near field measurements," Inverse Probl. Sci. Eng. **28** (3), 427–447 (2020).
16. Y. G. Smirnov, A. A. Tsupak, and M. Y. Medvedik, "Non-iterative two-step method for solving scalar inverse 3D diffraction problem," Inverse Probl. Sci. Eng. **28** (10), 1474–1492 (2020).
17. Y. G. Smirnov and A. A. Tsupak, "Direct and inverse scalar scattering problems for the Helmholtz equation in R^m," J. Inverse Ill-Posed Probl. **30** (1), 101–116 (2022).
18. E. Smolkin, Y. Smirnov, and M. Snegur, "Solution of the vector three-dimensional inverse problem on an inhomogeneous dielectric hemisphere using a two-step method," Computation **12** (11), 213 (2024).
19. A. N. Tikhonov and V. Ya. Arsenin, *Methods for Solving Ill-Posed Problems* (Nauka, Moscow, 1979) [In Russian].
20. R. O. Evstigneev and M. Y. Medvedik, "Reconstruction of inhomogeneities in a hemisphere from the field measurements," Lobachevskii J. Math. **40** (10), 1653–1659 (2019).
21. R. O. Evstigneev and M. Y. Medvedik, "Reconstruction of inhomogeneity parameters by measurements of near field outside the body," in *Nonlinear and Inverse Problems in Electromagnetics (PIERS 2017)*, Springer Proceedings in Mathematics and Statistics, Vol. 243, Ed. by L. Beilina and Y. Smirnov (2018), pp. 29–38.
22. A. O. Lapich and M. Y. Medvedik, "Microwave tomography method for solving the inverse problem on cylindrical bodies," Tech. Phys. Lett. **50**, 360–364 (2024).
23. A. O. Lapich and M. Y. Medvedik, "Method of generalized and combined computational grids for restoration of the parameters of inhomogeneities of a body based on the results of measurements of the electromagnetic field," Math. Models Comput. Simul. **16** (6), 806–813 (2024).
24. A. O. Lapich and M. Y. Medvedik, "Method for reconstruction the parameters of body inhomogeneities from the results of electromagnetic field measurements," Lobachevskii J. Math. **45** (10), 4740–4747 (2024).

Publisher's Note. Pleiades Publishing remains neutral with regard to jurisdictional claims in published maps and institutional affiliations.
AI tools may have been used in the translation or editing of this article.